

Can density based coal processing techniques be applied to fly ash beneficiation?

Robert Blissett

Department of Chemical Engineering, University of Birmingham, Edgbaston, B15 2TT, United Kingdom

KEYWORDS: Coal fly ash beneficiation, density separation, reflux classifier

ABSTRACT

The increasing interest in the multi-component utilisation of coal fly ash has provided a stimulus for examining new processing routes. Traditionally unburned carbon has been removed from fly ash using electrostatic separation or froth flotation. This paper looks at the theoretical possibility of using other systems that are often used for coal cleaning operations such as the hindered bed and reflux classifiers. In order to do so, products from an existing fly ash processing scheme are characterised with respect to bulk chemistry, particle size distribution, and density. These physico-chemical properties are used within literature models in order to assess the performance that the beneficiation equipment might be capable of. Recovery and grade of fly ash products are evaluated at different operating conditions. The results suggest that the newly applied processing equipment might be capable of a high degree of separation. This supports the view that simple density based separation techniques may be used in coal fly ash beneficiation. The analysis encourages further experimental work in order to verify its findings.

INTRODUCTION

Although the degree of accuracy may be questioned, current estimates show that 750 million tonnes of coal fly ash (CFA) are generated on a global basis each year; CFA utilisation figures are 39% in the US and 47% in Europe. The global average is estimated to be close to 25%¹. Thus it is clear that a significant proportion of the annual production of CFA is not currently being used to its full potential.

Current forecasts predict that the next two decades will see the installation of the same amount of power generation capacity as that installed over the whole of the 20th Century. Part of this increase in demand is likely to be fulfilled by renewable energy sources; however, due to its abundance in energy intensive countries such as China and India, coal is likely to become an increasingly dominant fuel for power generation². With demand for coal increasing, and CFA underutilised already, there exists a pressing requirement for new applications and technologies to be developed.

The concept of multi-component utilisation is not a new one; 3 review papers have summarised developments in this area over the last 15 years^{1,3-4}. The idea underpinning multi-component utilisation is that CFA is a heterogeneous material that contains

distinct fractions that can be separated to enhance both value and utility. As such a multi-stage processing scheme can produce a variety of materials: a lightweight fraction, often called cenospheres owing to their hollow spherical morphology; an enriched carbon component; a magnetic fraction; and two residual ash streams split into coarse and fine products⁵.

To successfully implement the concept of multi-component utilisation of CFA, new processing routes must be considered. Traditionally ash beneficiation has involved the removal of the organic component in order to lower Loss-on-Ignition (LOI) values to render the CFA suitable for classification as an Ordinary Portland Cement (OPC) substitute under American Society for Testing and Materials (ASTM) or European Standard guidelines. The most commonly used methods to lower the LOI value of CFA have been electrostatic separators, fluidised bed reactors, and froth flotation¹.

Increasing attention has been paid over the past 10 years to the possibility of cleaning fine low grade coal using hindered bed settlers⁶. The hindered bed settler operates with an upward flow of wash water against which a coal suspension settles. The bed operates at a high solids fraction which increases the suspension density and thus promotes partition of the less dense (relative to ash) coal particles to the overflow. The reflux classifier, recently developed at the University of Newcastle, Australia has also been used to clean fine coal⁷⁻⁸. The reflux classifier uses a set of inclined channels within a hindered bed type settler to suppress the effect of size on separation. The current study applies theoretical models for both the hindered and reflux classifier to a characterised CFA feed, to investigate the potential for utilising separators of this type as part of a CFA processing scheme.

THEORY

Hindered Bed Theory

A hindered bed settler, as shown in Figure 1, separates particles through the principles of particle dynamics. Settling particles settle against an apparent bed density and a rising wash water velocity. Particles having sufficient mass settle through the bed and report to the underflow. Those that don't, rise with the wash water, and report to the overflow. Hindered settling introduces an additional resistance to the falling particles. The particle slip velocity, U , may be expressed as a function of the solids volume fraction, Φ , the particle terminal velocity, U_T , and the Richardson-Zaki index, n^9 :

$$U = U_T(1 - \phi)^{n-1} \quad [1]$$

Equation [1] only strictly applies for materials that do not differ in density or size. Galvin et al.¹⁰ developed an empirical description for particle suspensions differing in both size and density which has been shown to match experimental data well. In a comparison study the Galvin slip velocity was found to match experimental data better than three other literature models¹¹.

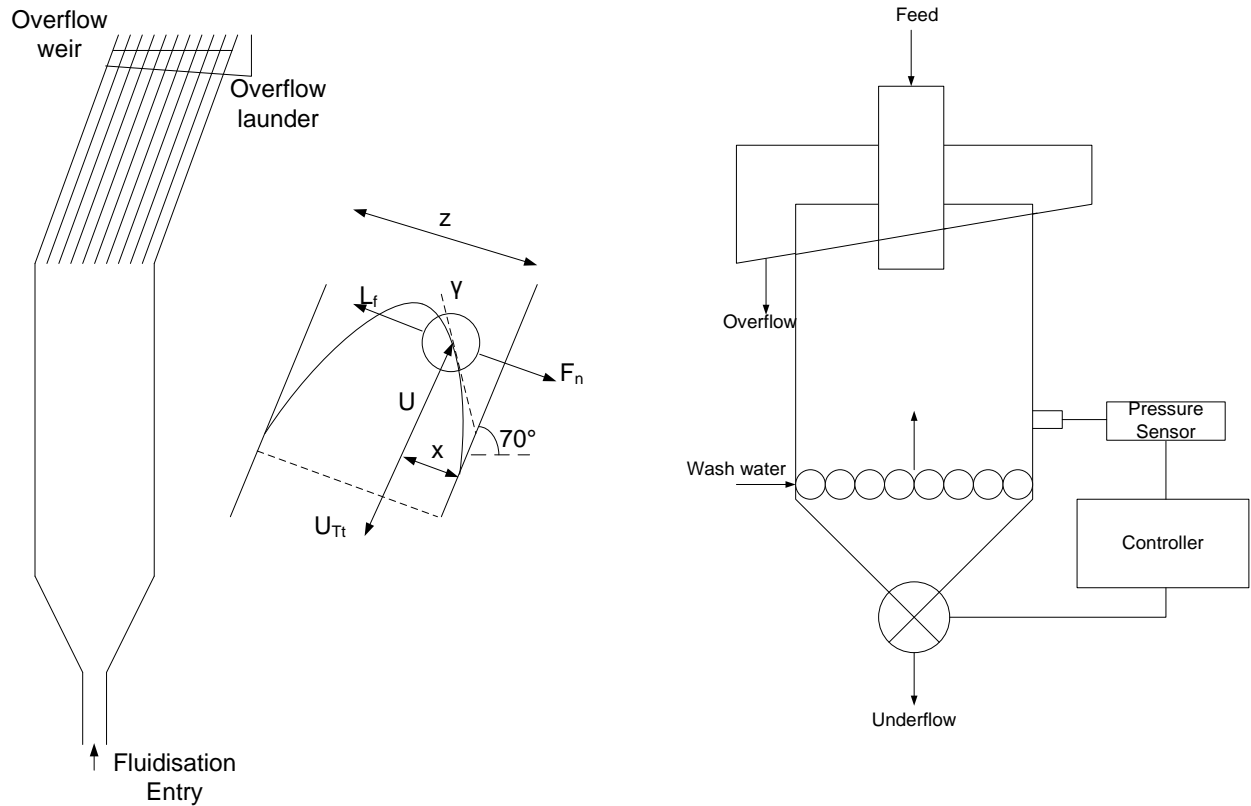


Figure 1 – Schematic of the reflux classifier and the inertial lift model for particles in the inclined channels (left - after⁸) and a hindered bed settler (right - adapted from⁶)

$$U_{ij} = U_{Tij} \left(\frac{\rho_{ij} - \rho_{sus}}{\rho_{ij} - \rho_f} \right)^{n_{ij}-1} \quad [2]$$

Where ρ is equal to the density: the subscripts i and j denote the size and density fractions of the feed respectively and the subscript f denotes the fluid. The average suspension density can be calculated according to equation [3].

$$\rho_{sus} = \sum \phi_{ij} \rho_{ij} + (1 - \sum \phi_{ij}) \rho_f \quad [3]$$

The terminal velocity for a single particle can be calculated across for particle Reynolds numbers $< 2 \times 10^5$ to a high degree of accuracy according to the following correlation for the drag coefficient C_D in terms of a dimensionless grain diameter, $d^* = (\Delta g / \nu^2)^{1/3} d$ where $\Delta = (\rho_s - \rho) / \rho$, g is the acceleration due to gravity, ν is the kinematic viscosity of the fluid, ρ is the density of the fluid, and ρ_s is the density of the grain¹². The dimensionless settling velocity $U_T^* = (\Delta g \nu)^{-1/3} U_T$ can then be calculated from $U_T^* = [4d^* / (3C_D)]^{0.5}$.

$$C_D = \frac{432}{d^{*3}} (1 + 0.022d^{*3})^{0.54} + 0.47 [1 - \exp(-0.15d^{*0.45})] \quad [4]$$

Estimation of the Richardson-Zaki index may be made using the following expression as a function of the particle Reynolds number¹³.

$$n_{ij} = \frac{2(2.35+0.175Re_T^{0.75})}{(1+0.175Re_T^{0.75})} \quad [5]$$

$$Re_T = \frac{d\rho U_T}{\mu} \quad [6]$$

ρ and μ are the density and dynamic viscosity of the fluid respectively.

Reflux Classifier Theory

The reflux classifier is represented schematically in Figure 1. The fluidized bed consists of an inclined section in which closely spaced inclined channels are placed. These channels have the effect of suppressing the role that size plays in elutriation and as such provide a cleaner cut when separating particles according to their density. A detailed description of the reflux classifier is provided by Galvin et al⁷.

The inertial lift model for the particle hydrodynamics within the reflux classifier was developed and validated experimentally by Galvin and Liu⁸ for low volume fraction suspensions of differing densities. Figure 1 shows a planar channel of spacing z , inclined at 70° to the horizontal. A particle of diameter d is a distance x away from the upwards facing channel wall exposed to a superficial velocity U . If the flow is laminar then the local velocity U impinging on the particle is given by Equation [7].

$$U = \frac{6U'x}{z} \left(1 - \frac{x}{z}\right) \quad [7]$$

The critical condition for elutriation is satisfied when the local velocity U which varies with x is equal to the particle terminal velocity in the tangential direction U_{Tt} .

A second constraint on the particle is applied in order to find its equilibrium distance x from the upwards channel wall. Equation [8] is used to determine if the particle lifts due to inertia from the channel surface⁸.

$$J = \frac{Re_s^2}{Re_{Tn}} > 32 \quad [8]$$

The shear Reynolds number is given by $Re_s = \rho\gamma d^2/\mu$ where γ is the shear rate. The particle Reynolds number $Re_{Tn} = \rho U_{Tn}d/\mu$ where U_{Tn} is the particle terminal velocity normal to the inclined surface. The shear rate is given by differentiating Equation [7].

$$\gamma = \frac{6U'}{z} \left(1 - \frac{2x}{z}\right) \quad [9]$$

If the constraint in Equation [8] is met then the particle lifts away from the wall and as it does so experiences a lower shear rate. Equilibrium is reached when the value of J is equal to 32.

In order to apply the inertial lift model to the higher volume fractions required for density separation of CFA, Equation [2] was applied to the terminal velocities calculated using Equation [4] to reflect the hindered settling that would occur. In the normal direction the acceleration due to gravity is replaced by $g\cos(\theta) = 3.352 \text{ ms}^{-2}$. In the tangential direction it is replaced by $g\sin(\theta) = 9.209 \text{ ms}^{-2}$. For both cases the angle of inclination is set at 70° ⁸.

METHODS

The materials were characterized with respect to their particle size distribution, shape, and density. The particle density was obtained with either a Micrometrics AccuPyc II helium pycnometer, in which the average density was taken over 3 cycles, or a specific gravity bottle. The particle size distribution was measured using a Malvern Mastersizer 2000 laser diffraction analyser. The suspensions of particles were diluted with water and placed in an ultrasonic bath for 10 minutes prior to analysis to breakdown any agglomeration. A refractive index of 1.65 and an absorption index of 0.1 were used in the calculation model. The morphology of the two samples was examined using a Philips XI30 scanning electron microscope (SEM) with a LaB6 filament emission source. The samples were mounted on specimen stubs with carbon tape and coated with carbon prior to imaging. The bulk chemistry of the raw CFA feed was determined using X-ray fluorescence spectroscopy (XRF), with samples prepared by a lithium borate fused bead method. The Loss-on-ignition (LOI) tests were performed in a furnace at 1000°C for 2 hours to measure the carbon content of the ashes.

MATERIALS

Raw CFA and processed components of CFA were obtained from the ash processing company RockTron Ltd (UK). The raw CFA was supplied from the Ferrybridge power station and the processed materials were supplied from RockTron's pilot plant in Gale Common: both in the UK. The processed materials obtained included an enriched carbon material (carbon), an enriched magnetic material (magnetite), and a low density hollow micro spherical material (cenospheres).

Figure 2 shows the morphology of the processed CFA materials. There are varying degrees of sphericity: the cenospheres appear almost perfectly spherical; the magnetite has a high degree of sphericity from the frame of view but there is some irregularity present; the raw CFA has a large number of smaller spheres but also some irregular large particles; and the carbon is predominantly irregular in shape and appears to be highly porous. Although an assumption of spherical particles is far from the complete picture as evidenced by the SEM analysis, for the purposes of further modeling work it is deemed sufficient.

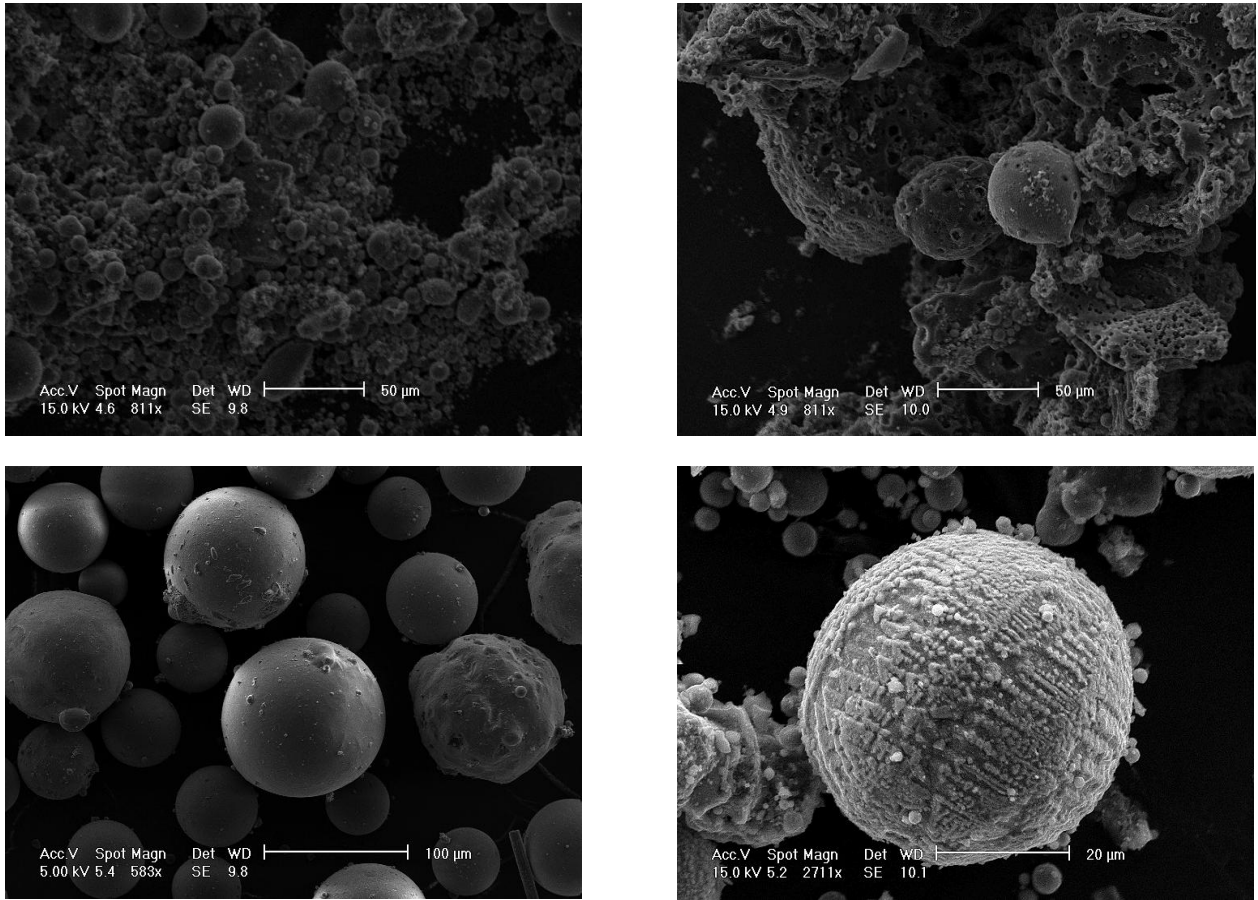


Figure 2 – SEM images showing the morphology of (top left) – raw CFA, (top right) – carbon, (bottom left) – cenospheres, and (bottom right) - magnetite¹

Density (SG)			
Carbon	Raw CFA	Magnetite	Cenospheres
1.4	2.2	3.5	0.8

Table 1 – Specific gravity of the processed CFA materials and raw CFA as determined by gas pycnometry and specific gravity bottle

The specific gravity results in Table 1 illustrate the density differences between the different components ranging from the low density cenospheres to the high density magnetite.

The bulk chemical composition of the raw CFA shown in Table 2 allows an assumption to be made on the relative compositions of the four separable components to be modeled. For the purposes of further modeling it is assumed that all of the Fe_2O_3 resides in the magnetite phase and is extractable. Similarly all the LOI content is assumed to be extractable in the carbon phase. The cenosphere composition is found from a sink float test in water to be around 1% of the feed CFA. The ash content is then assumed to be equal to unity minus the sum of the other three mass fractions. This assumption is highly simplistic but for the purposes of this study is deemed appropriate.

SiO ₂	Al ₂ O ₃	Fe ₂ O ₃	CaO	K ₂ O	MgO	TiO ₂	Na ₂ O	P ₂ O ₅	MnO	LOI
48.5	25.5	10.5	2.6	2.8	1.6	1.0	0.5	0.3	0.1	6.8

Table 2 – Bulk chemical composition of raw CFA as determined by XRF and LOI at 1000°C

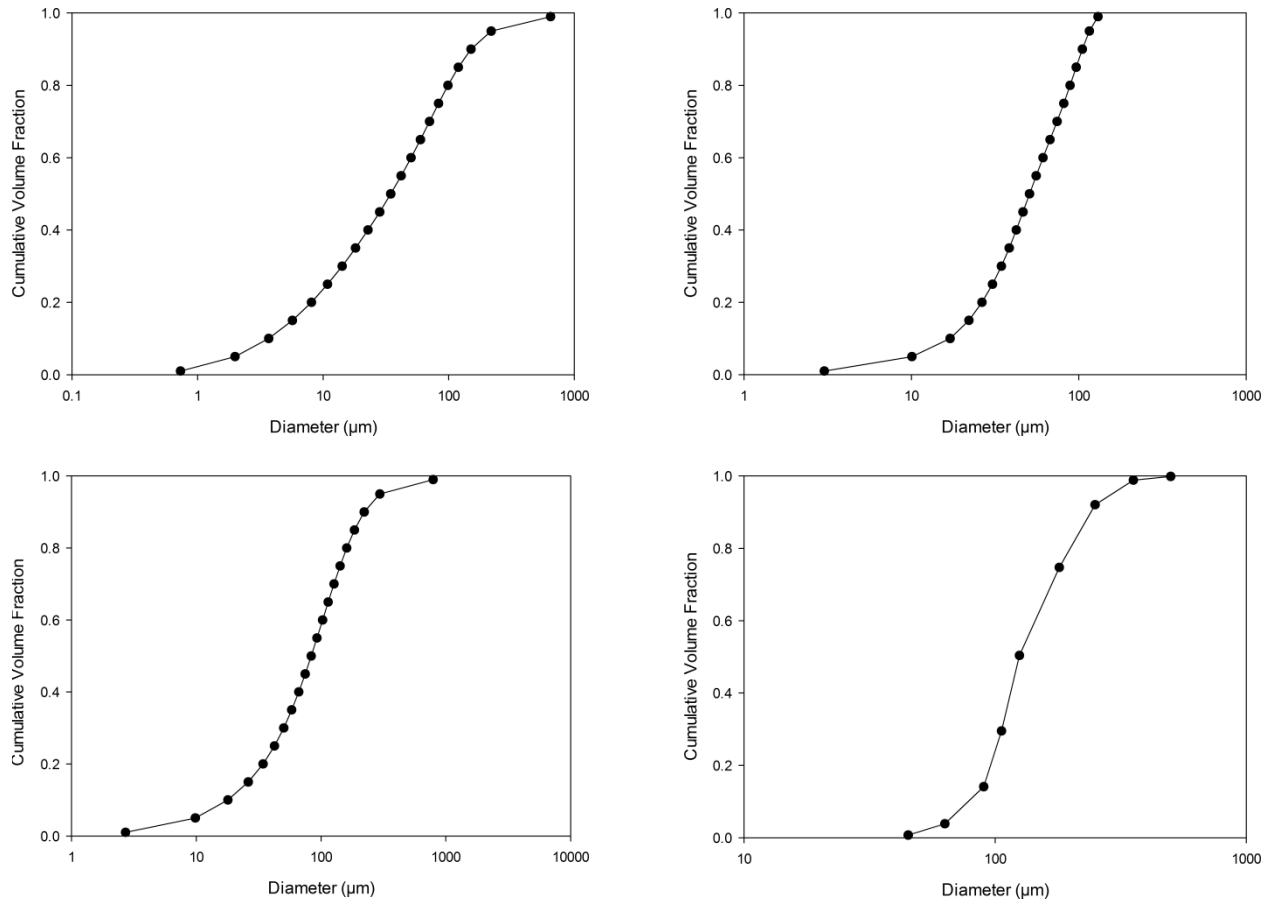


Figure 3 – Particle size distribution of (top left) – raw CFA, (top right), - magnetite, (bottom left) – carbon, and (bottom right) – cenospheres

Figure 3 shows the particle size distribution of the 4 materials studied. In general the cenospheres and carbon are larger than the feed CFA while the magnetite is smaller. This should make the separation by density a little more challenging because the larger carbon particles are likely to be displaced to the underflow, while on the other hand, the smaller magnetite particles have the potential to be displaced to the overflow.

COMPUTATION

The computation methods in this study are broadly aligned with the procedure used in previous studies^{6,11}. The computation occurs in a combination of an excel spreadsheet with additional VBA code.

Feed Composition

The feed is divided into 4 different densities j . The mass fraction of each density is based on the bulk chemical composition analysis along with a sink float analysis for the

cenosphere fraction. The residual ash is assumed to have the same properties as the raw CFA. For each density fraction the particle size at each decile is taken from the raw particle size distribution data and then interpolated to obtain particle size at each percentile of the cumulative size distribution. The particle size mass fractions are multiplied by the density mass fraction to give overall mass fraction of the feed material. An array of (4, 100) unique size and density combinations is produced. By adhering to the overall and component mass balances each combination is tracked over the separation process. In both unit operations the cenospheres, with a density less than that of water, are assumed to report to the overflow regardless of operating parameters.

Hindered Bed Calculations

The slip velocity of each component of the particle array is compared to the superficial water velocity divided by the bed voidage. If the particle has a slip velocity greater than the wash water velocity it reports to the underflow and if it has a slip velocity less than the wash water velocity it reports to the overflow. All array components are tracked and placed into underflow and overflow holders from where stream compositions and partitions can be calculated.

Reflux Classifier Calculations

The particle terminal velocities are calculated in both the normal and tangential directions. The slip velocity is calculated based on these, assuming solids volume fraction in the inclined channels is the same as in the fluidized bed. The particle is at first assumed to reside at the surface such that $x = d/2$. Equation [7] is rearranged to give the superficial velocity U' with $U = U_{Tt}$. The shear stress is then calculated from Equation [9] and used to evaluate the constraint in Equation [8]. If J is greater than 32 then the particle will lift from the wall and the equilibrium position $x = d/2$ is incorrect. In this case the goal-seek function within Excel is used to calculate the equilibrium position of the particle at $J = 32$. The resulting tangential velocity is again equated to the local velocity U and the superficial velocity is calculated giving the velocity required for elutriation.

RESULTS AND DISCUSSION

Hindered Bed Settler

A series of simulations were carried out to model a hindered bed settler at different solids loadings, represented here by suspension density, and superficial water velocities. Figure 4 shows the hindered settling velocity as a function of particle diameter; the dotted line represents the interstitial water velocity. Everything above this line will settle to the underflow and all particles below this line will carry into the overflow. It is obvious from this plot that even at a low water velocity of 1 mm/s significant proportions of the magnetite and ash are carried over into the overflow. The cut sizes are around 35 μm and 60 μm for the magnetite and the ash respectively.

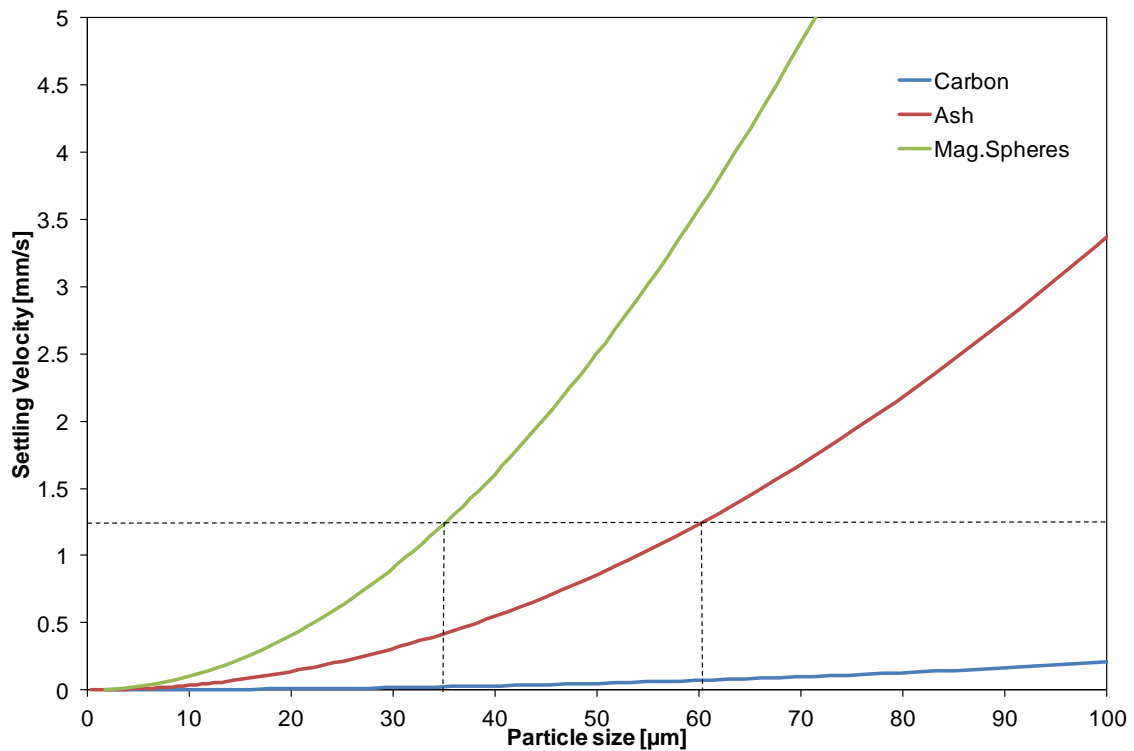


Figure 4 – Settling velocity as a function of particle size for a hindered bed settler operating at a suspension density of 1192 kg/m³. Dotted line represents the interstitial velocity and the cut size at this velocity.

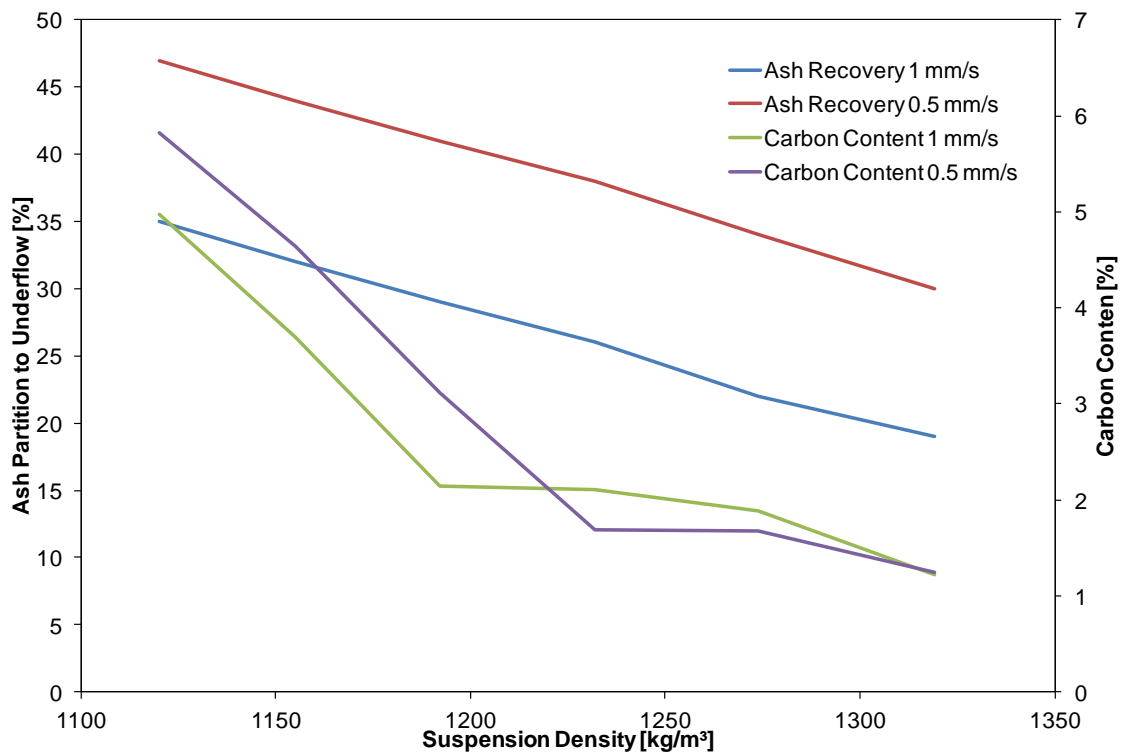


Figure 5 – Ash recovery in the underflow and carbon content in the underflow as a function of suspension density at a superficial water velocity of 1 mm/s and 0.5 mm/s.

FEED PARTITION (Component %)		
Component	Overflow	Underflow
Spheres	100	0
Carbon	90	10
Ash	71	29
Mag.Spheres	30	70

Table 3 – Partition of the various components in the feed CFA to underflow or overflow in a hindered bed settler with a water velocity of 1 mm/s and a suspension density of 1192 kg/m³.

If the objective of the separation is the removal of carbon, then the recovery of ash to the underflow is a key outcome. Figure 5 shows the ash recovery and carbon content of the feed as a function of the suspension density for a water flow rate of 1 mm/s. Firstly it is to be noted that ash recovery is not particularly high in any of the cases. This notwithstanding, there is a classic trade-off apparent: as the recovery decreases so does the carbon content. Reducing the water flow rate to 0.5 mm/s does increase the recovery but in terms of velocity required for fluidization this is probably as low as the system can operate at. It is also to be noted that with such low water velocity rates overflow flux will be affected.

There are other possibilities to utilize a separator of this kind in an ash processing circuit other than for primary carbon removal. Table 3 shows the partition of all of the components to the overflow or underflow of the separator. It is clear that under the operating conditions specified, 70% of the magnetic fraction has been removed in the underflow as well as 29% of the coarser ash particles. This would have the effect of reducing the size of downstream processing units such as froth flotation tanks and removing some of the less valuable coarse ash fractions; the utility of this however, is probably not high enough to warrant the capital investment in what would essentially be a pre-processing step.

Reflux Classifier

The reflux classifier simulations were carried out over a range of different suspension densities (1120-1274 kg/m³) and channel wall spacings (2-8 mm). The upper limit on the channel spacing is applied because larger channel spacing is likely to result in turbulent conditions under which the inertial lift model cannot be applied⁸.

With a small channel width, it is evident from Figure 6 that there is a strong segregation effect due to density. The elutriation velocity for carbon particles remained extremely low for particle diameters up to 500 µm. This is explained by the common elutriation condition that the particles are exposed to. The fine particles reside at the channel walls and they are exposed to a velocity gradient depending on their position, x , away from the wall. The larger the particle, the higher the velocity they are exposed to and thus particles of the same density, but different sizes are elutriated at the same operating conditions. This phenomenon is not so evident for the heavier magnetite particles but for the ash particles the elutriation velocity gradient is not as steep. What is noticeable,

is that for ash particles around 250-300 μm in diameter the particles start to experience an inertial lift away from the channel walls and the “nose” feature observed in the original modeling study⁸ can be observed. This occurs because the heavier particles experience a lift force greater than the net weight of the particle normal to the surface. They move further away from the wall and so experience an even higher elutriation velocity.

As the channel spacing increases to 8 mm, the size appears to play more of a role for all of the particles considered. Figure 7 shows that the ash and magnetite elutriation velocity gradient now rise steeply with increasing diameter. However, although the carbon is affected by an increase in gradient of its velocity curve it is not anywhere to the same extent. This suggests that at these conditions, the separation for this particular system might actually be more favorable than with a smaller channel.

The ash recovery to the underflow for a wider channel is in fact increased as has been suggested above. Figure 8 shows ash recoveries as high as 86% at a suspension density of 1120 kg/m^3 and a channel width of 8 mm. This is largely due to the fact that at a given shear rate, the superficial velocity required to achieve a given separation increases. Therefore, for the wider channels more ash is able to settle against the same reflux water velocity because of the higher elutriation velocity. This is beneficial if what is required is the retention of the ash in the underflow.

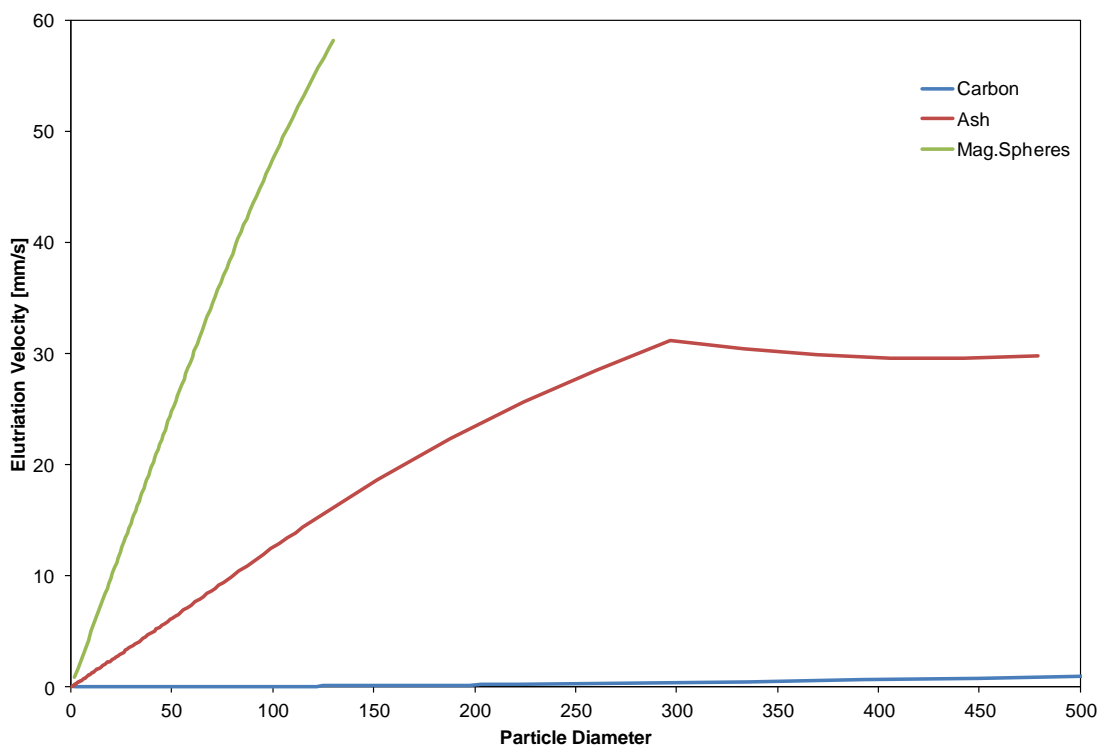


Figure 6 – Elutriation velocity as a function of particle diameter for a reflux classifier with channel width 2 mm, operating at 1192 kg/m^3

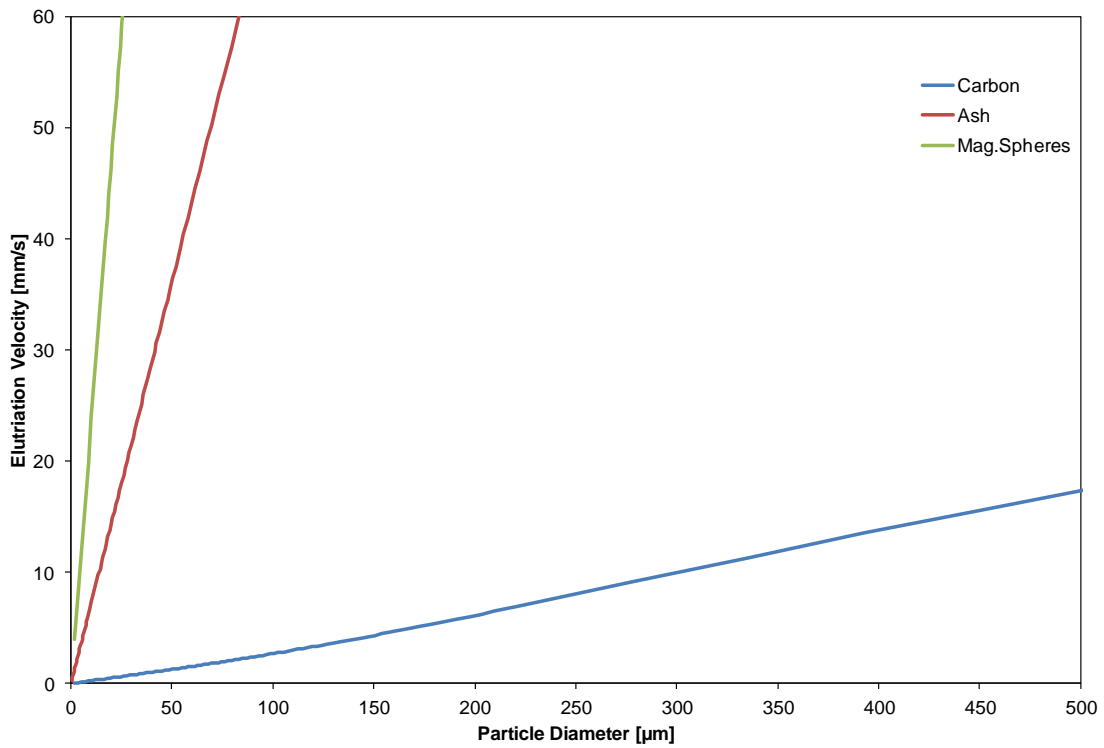


Figure 7– Elutriation velocity as a function of particle diameter for a reflux classifier with channel width 8 mm, operating at 1192 kg/m³

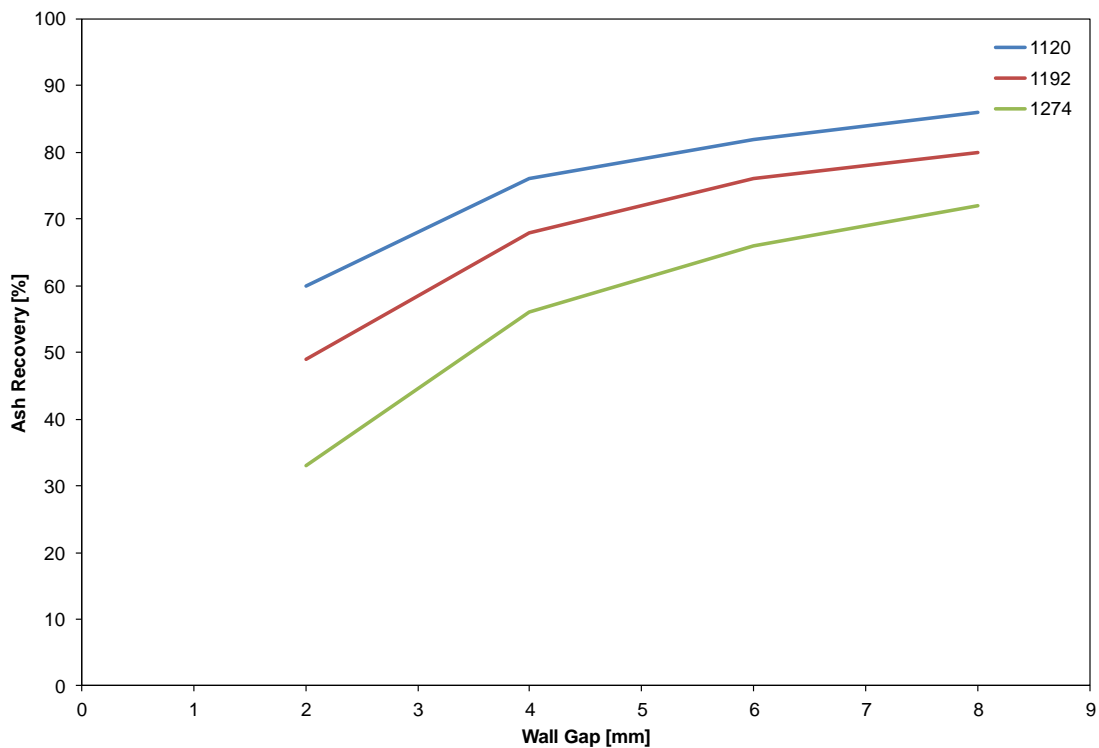


Figure 8 – Ash recovery to underflow as a function of wall gap for a water velocity of 5 mm/s. Numbers in the key refer to suspension density.

Figure 8 and Figure 9 show that for the intermediate suspension density of 1192 kg/m³, a recovery of 80% ash and a carbon content of around 1.3% is possible in the underflow product, with a channel width of 8 mm and a water velocity of 5 mm/s. Even at the lowest suspension density with the highest recovery rates of 86%, a reduction in carbon content to around 5% is possible.

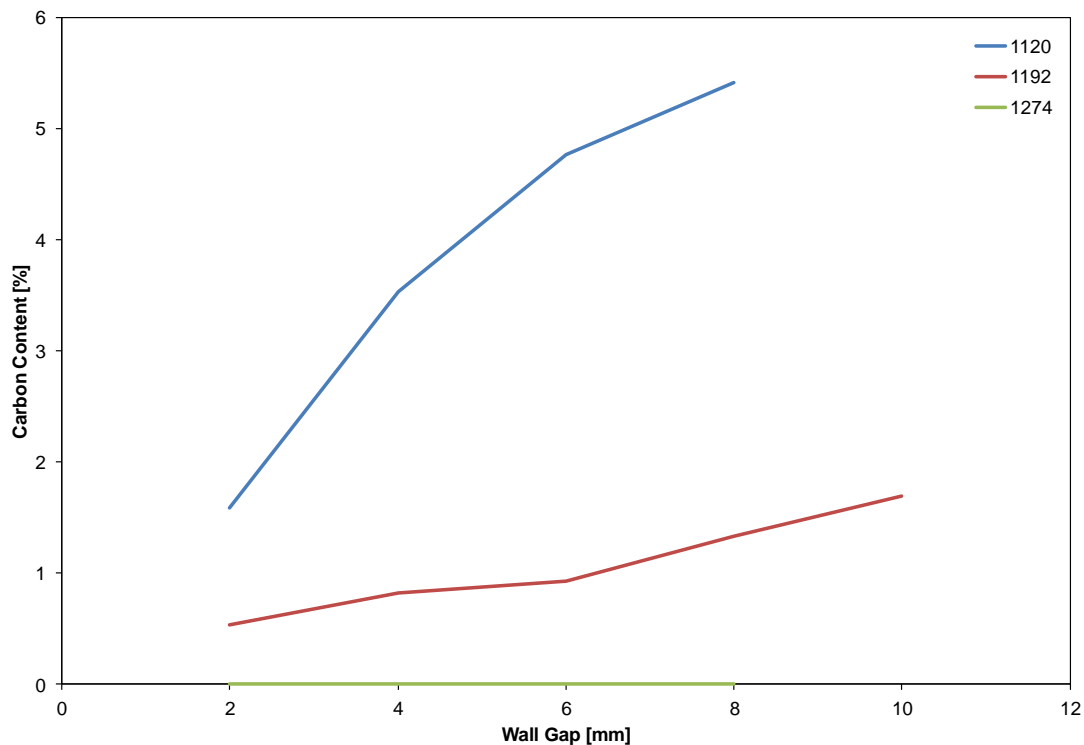


Figure 9 – Carbon content of underflow product as a function of wall gap for a water velocity of 5 mm/s. Numbers in key refer to suspension density.

For the “best” case considered under the conditions simulated in this study it is clear from Table 4 that the reflux classifier has significant potential to beneficiate CFA. It is capable of removing, 100% of the spheres and 85% of the carbon with only 20% of the ash and 1% of the magnetite to the overflow. This allows for a significant reduction in demand for any carbon concentrating processes downstream. The major issue with this approach is that the ash that does elutriate is comprised of the finer, more valuable fraction.

FEED PARTITION (Component %)		
Component	Overflow	Underflow
Spheres	100	0
Carbon	85	15
Ash	20	80
Mag.Spheres	1	99

Table 4 - Partition of the various components in the feed CFA to underflow or overflow in a reflux classifier with a water velocity of 5 mm/s, a suspension density of 1192 kg/m³ and a channel width of 8 mm.

CONCLUDING REMARKS

It is fairly evident from the above that neither of these models has been validated against experimental results. In order to have any confidence in the results that have been produced above this must be done as the prioritized next step in research. There are also a number of significant assumptions that have been made which limit the results to be considered an ideal case: the three most important of these are (1) that there exists no displacement of particles to the wrong outlet through entrainment or some other cause; (2) that from the bulk chemical composition the mass fraction of separable components can be inferred; and (3) that the components do not vary in density – in reality there will most likely be a mass density distribution for each component that will either aid or hinder separation.

Despite the acknowledged weaknesses of this study it can be concluded that the hindered bed settler is unlikely to form part of a CFA processing flow sheet for the CFA characterized. On the other hand the reflux classifier has significant potential to be used for the processing of CFA. In various different configurations it is likely to be capable of achieving different objectives. As such an experimental study of its potential should be the next logical step.

REFERENCES

- [1] Blissett, R. S. & Rowson, N. A. A review of the multi-component utilisation of coal fly ash. *Fuel* 97, 1-23 (2012).
- [2] Lior, N. Sustainable energy development: The present (2009) situation and possible paths to the future. *Energy* 35, 3976-3994 (2010).
- [3] Vassilev, S. V., Menendez, R., Alvarez, D. & Borrego, A. G. in *International Ash Utilization Symposium*. (2001). Centre of Applied Energy Research, University of Kentucky
- [4] Nugteren, H. W. Coal Fly Ash: From Waste to Industrial Product. *Part Part Syst Char* 24, 49-55 (2007).
- [5] Blissett, R. S. & Rowson, N. A. An Empirical Model for the Prediction of the Viscosity of Slurries of Coal Fly Ash with Varying Concentration and Shear Rate at Room Temperature. Manuscript submitted for publication (2013).
- [6] Das, A., Sarkar, B. & Mehrotra, S. P. Prediction of separation performance of Floatex Density Separator for processing of fine coal particles. *International Journal of Mineral Processing* 91, 41-49 (2009).
- [7] Galvin, K. P., Walton, K. & Zhou, J. How to elutriate particles according to their density. *Chem Eng Sci* 64, 2003-2010 (2009).

- [8] Galvin, K. P. & Liu, H. Role of inertial lift in elutriating particles according to their density. *Chem Eng Sci* 66, 3687-3691 (2011).
- [9] Richardson, J. F. & Zaki, W. N. Sedimentation and fluidisation: Part I. *Transactions of Institution of Chemical Engineers* 32, 35-53 (1954).
- [10] Galvin, K. P., Pratten, S. & Nguyen Tran Lam, G. A generalized empirical description for particle slip velocities in liquid fluidized beds. *Chem Eng Sci* 54, 1045-1052 (1999).
- [11] Sarkar, B. & Das, A. A comparative study of slip velocity models for the prediction of performance of floatex density separator. *International Journal of Mineral Processing* 94, 20-27 (2010).
- [12] Cheng, N.-S. Comparison of formulas for drag coefficient and settling velocity of spherical particles. *Powder Technology* 189, 395-398 (2009).
- [13] Rowe, P. N. A convenient empirical equation for estimation of the Richardson-Zaki exponent. *Chem Eng Sci* 42, 2795-2796 (1987).